



Removal of cationic dyes by poly(AA-co-AMPS)/montmorillonite nanocomposite hydrogel

Hossein Hosseinzadeh^{a,*}, Neda Khoshnood^b

^aChemistry Department, Payame Noor University, 19395-4697 Tehran, Iran, Tel. +98 44 45227777; Fax: +98 44 45227997; email: h_hosseinzadeh@pnu.ac.ir

^bFaculty of Science, Chemistry Department, Urmia University, Urmia, Iran, Tel. +98 44 32752740; email: khoshnoodneda@gmail.com

Received 7 July 2014; Accepted 9 January 2015

ABSTRACT

In this work, adsorption feasibility of a cationic dye, methylene blue (MB), onto an anionic hydrogel nanocomposite was investigated in detail. Firstly, the hydrogel nanocomposite was synthesized via a simple solution copolymerization of acrylic acid and 2-acrylamido-2-methylpropanesulfonic acid monomers in the presence of montmorillonite (MMT) by using ammonium persulfate as an initiator and methylene bisacrylamide as a crosslinker. Then, the effects of agitation time, MMT content, pH, initial dye concentration, adsorbent dose, and temperature were optimized with respect to the dye adsorption capacity of nanocomposites. The thermodynamic parameters such as changes in standard free energy, enthalpy, and entropy demonstrated that dye adsorption onto the hydrogel nanocomposite was spontaneous and endothermic, and especially more effective at high temperatures. Moreover, the results indicated that the equilibrium adsorption isotherm data of the hydrogel nanocomposite better fit to the Redlich–Peterson than to the Langmuir, Freundlich, and Temkin models. The experimental results also fit to pseudo-first-order, pseudo-second-order, and intraparticle diffusion kinetic models. The results indicated that the adsorption of MB followed pseudo-second-order kinetics.

Keywords: Hydrogel; Nanocomposite; Montmorillonite; Adsorption; Methylene blue

1. Introduction

Several industries, such as textile, cosmetics, leather, paper, and plastic, use various dyes in order to color their products which generate large amounts of colored wastewater. These synthetic dyes cause considerable environmental pollution. Therefore, dye removal from wastewaters is a research area of increasing interest due to environmental importance. Among the numerous physical, chemical, and biological

methods of dye removal, adsorption process is one of the most suitable and superior technique for decolourization of wastewaters because of its simplicity and regeneration capability [1–8]. In this regard, many adsorbents had been used previously such as agriculture and industrial waste materials, naturally available inorganic minerals, and bioadsorbents. Sharma et al. in a review reported an extensive list of adsorbents obtained from different sources [9]. Some of the reported adsorbents for the elimination of residual dyes from wastewaters were summarized in Table 1.

*Corresponding author.

Table 1
Some of the most used adsorbent materials for the adsorption of various dyes

Adsorbent type	Example	Dye	References
Agriculture waste materials	Activated carbon	Congo red	[37]
	Rice husk	MB	[38]
	Wheat barn	Remazol red F3B	[39]
	Sludge ash	MB	[40]
Fruit wastes	Orange peel	Direct red 23	[41]
	Banana pith	Methyl orange	[42]
	Olive pomace	Reactive red 198	[43]
	Jack fruit peel	Basic blue 9	[44]
Plant wastes	Activated desert plant	MB	[45]
	Sawdust	Methylene violet	[46]
	Jute stick powder	Rhodamine B	[47]
	Sawdust-oak	Acid blue 25	[48]
Natural inorganic materials	Sepiolite	Reactive blue 221	[49]
	Zeolite	Reactive red 239	[50]
	Perlite	Methyl violet	[51]
	Modified bentonite	Crystal violet	[52]
Bioadsorbents	Cellulose	Reactive Blue 2	[30]
	Alginate	Crystal violet	[53]
	Chitosan	Acid red 18	[54]
	Chitin	Reactive yellow 2	[55]

Hydrogels, which have been used as an adsorbent in this work, are three-dimensional polymeric networks capable of imbibing large quantities of water in their structures [10]. Polymer hydrogels have gained biomedical applications due to their unique water absorption along with its retention capacity [11–13]. The use of hydrogels, however, is restricted in some applications because of their poor stability and mechanical properties. Polymer/clay nanocomposite hydrogels have been studied to improve these properties of hydrogels [14–18]. These materials are commonly defined as combination of polymer matrix and additives that have at least one dimension in the nanometer range. Among clays, montmorillonite (MMT) was extensively used as a reinforcing filler in the preparation of hydrogel nanocomposites [19,20].

In this work, poly(acrylic acid-co-2-acrylamido-2-methylpropanesulfonic acid) hydrogel nanocomposite as an anionic adsorbent was tested to remove methylene blue (MB) as a cationic dye. The molecular structure of MB dye is depicted in Fig. 1.

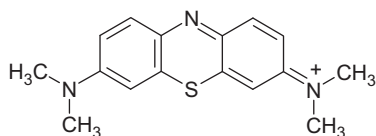


Fig. 1. The chemical structure of MB.

2. Experimental

2.1. Materials

Acrylic acid (AA, from Fluka), 2-acrylamido-2-methylpropanesulfonic acid (AMPS, from Merck), methylene bisacrylamide (MBA, from Fluka), ammonium persulfate (APS, from Merck), and sodium montmorillonite (NaMMT, from Southern Clay) were of analytical grade. The basic dye, MB, was obtained from Sigma-Aldrich and used without purification. Distilled water was used for preparation of all experimental solutions.

2.2. Preparation of adsorbent

The hydrogel nanocomposites were prepared via a simple free-radical copolymerization. The feed compositions and reaction conditions are listed in Table 2. Briefly, certain amounts of AA (2.0 mL) and AMPS (2.0 g) monomers were added to a three-neck reactor equipped with a mechanical stirrer (Heidolph RZR 2021, three blade propeller type, 300 rpm) including 30 mL double-distilled water. The reactor was immersed in a thermostated water bath preset at 70 °C. After 15 min, an appropriate weight of the MMT nanopowder (0.1–1.0 g) was added to the reaction mixture and was stirred for 120 min. Then, a definite amount of APS solution (0.1 g dissolved in 1 mL H₂O) was added to solution. After adding APS initiator,

Table 2

Feed compositions and preparation conditions for the hydrogel nanocomposites

Sample code	Feed components					Reaction temperature (°C)	Reaction time (h)
	AA (mL)	AMPS (g)	MMT (g)	MBA (g)	APS (g)		
S0	2	2	0	0.05	0.1	70	3
S1	2	2	0.1	0.05	0.1	70	3
S2	2	2	0.5	0.05	0.1	70	3
S3	2	2	1.0	0.05	0.1	70	3

methylene bisacrylamide solution (0.05 g dissolved in 1 mL H₂O) was added to the reaction mixture. After 180 min, the reaction product was allowed to cool to ambient temperature and neutralized to pH 8 by addition of 1 M sodium hydroxide solution. The hydrogel was poured into excess non-solvent ethanol (200 mL) and kept for 3 h to remove absorbed water. Then ethanol was decanted and the product was cut to small pieces. Again, 100 mL of fresh ethanol was added and the hydrogel nanocomposite was stored for 24 h. Finally, the filtered product was dried in an oven at 60°C for 10 h. After grinding by mortar, the powdered hydrogel nanocomposite was stored by protecting from moisture, heat, and light.

2.3. Batch adsorption experiments

Dye adsorption experiments were carried out at 25°C using a batch technique. Adsorption studies were conducted at 400 rpm by mechanical agitation for 10 h. The hydrogel nanocomposites (0.1 mg) were added into 50 mL of dye solution. The amount of residual dye in the solution at any time was determined from absorbency as measured using a UV–Vis spectrophotometer (Perkin-Elmer Lambda 35) at 664 nm, which was the maximum wave length for MB dye.

The adsorption capacity (q_e) of the hydrogel nanocomposites was calculated by using the following equation:

$$q_e = \frac{(C_0 - C_e) \times V}{W} \quad (1)$$

where q_e (mg g⁻¹) is the amount of dye adsorbed by hydrogel nanocomposite, C_0 (mg L⁻¹) is the initial concentration of MB in the solution, C_e (mg L⁻¹) is the equilibrium concentration of MB in the solution, V (L) is the initial volume of the dye solution, and W (g) is the dry weight of the hydrogel nanocomposite.

It should be pointed out that in dye adsorption experiments using hydrogels; however, water

molecules will also be adsorbed in addition to dissolved dye molecules. This method for dye absorbency measurements is a well-known simple method to evaluate the absorbency. This method is given in most of the hydrogel-related reports [1,2]. Swelling of hydrogel in water leads to an enhanced removal of dye molecules. However, for the application of the synthesized hydrogels on industrial scale, water molecules should be removed. For this purpose, the swelled hydrogel was generally immersed in excess of non-solvent ethanol for 24 h and therefore the adsorbed water molecules were removed by ethanol. Moreover, this “dewatering” can be a kind of “purifying” if the impurities are totally water-soluble and the dewatered particles are as small as possible. Since our product or procedure (scissoring to small pieces) has the mentioned specifications, we are sure about the efficiency of our purification method.

3. Results and discussion

3.1. Adsorbent synthesis

The main goal of this study is to synthesize a novel anionic copolymer hydrogel nanocomposite adsorbent for removal of cationic MB from aqueous solutions. Acrylic acid and 2-acrylamido-2-methylpropanesulfonic acid as anionic monomers were copolymerized in the presence of an initiator and a crosslinker (Fig. 2). Sodium MMT as nanofiller reinforcement was also intercalated within the hydrogel network resulting in hydrogel nanocomposite.

The prepared negatively charged hydrogel nanocomposite comprising carboxylate and sulfate functional groups leads to electrostatic interactions with the positively charged MB dye molecules as shown in Fig. 3.

3.2. Effect of contact time on dye adsorption capacity

Fig. 4 shows the effect of agitation time on the MB adsorption. It is observed that the uptake of dye onto the hydrogel (S0) and the hydrogel nanocomposites

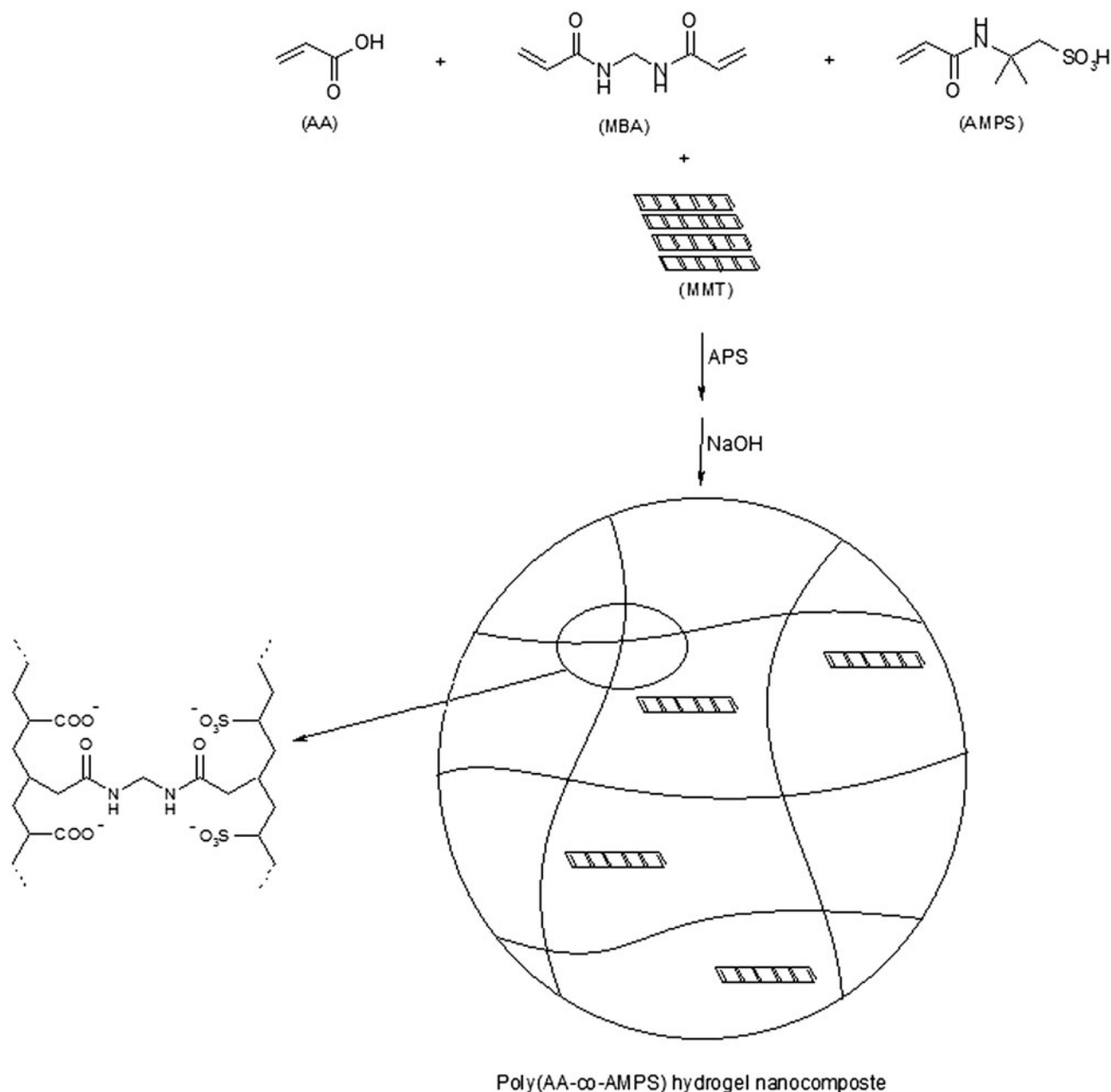


Fig. 2. Schematic illustration of the formation of hydrogel nanocomposite.

(S1, S2, and S3) increased with contact time. It is obvious that increase in reaction time provides better opportunity for interaction between the adsorbent and the adsorbate. Moreover, the hydrogel nanocomposites have higher adsorption capacity than the hydrogel sample. This may be due to the negative charges in the hydrogel nanocomposites. In fact, nanoclays are already reported as good adsorbents for various materials due to its large specific surface area and high negative charge density [21]. So strong interactions

between MMT layers and hydrogel nanocomposite network will be affecting the adsorption capacity. Furthermore, the incorporation of low amount of clay into the hydrogel increased the absorbency due to hydrophilic surfaces of MMT [22]. But the lower dye adsorption capacity of sample S3 can be attributed to the higher content of MMT nanoclay (see Table 2). In fact, high MMT content in sample S3 decreases the swelling capacity and therefore the adsorption ability due to the crosslinking role of nanoclays [23]. This

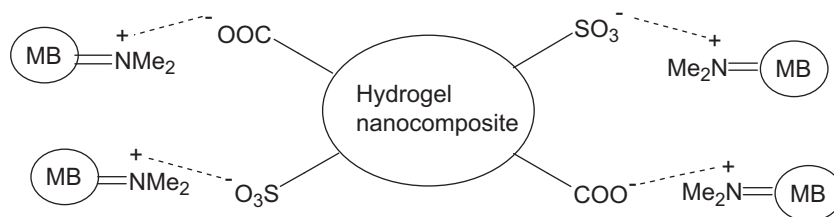


Fig. 3. Electrostatic interactions between negative and positive functional groups of hydrogel nanocomposite and MB dye molecules.

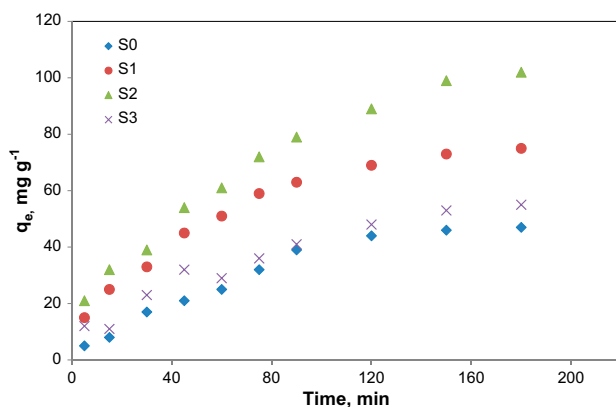


Fig. 4. Effect of contact time on MB adsorption.

trend (adsorption capacity: $S2 > S1 > S3 > S0$) was observed when the effect of other parameters on adsorption behavior was considered.

3.3. Effect of pH on dye adsorption capacity

The synthesized hydrogel nanocomposites are comprised of sulfate and carboxylate functional groups, which are affected by the pH of the dye solution. So the effect of pH as an important parameter on the adsorption capacity was investigated (Fig. 5). The increase in MB removal was observed when pH was increased from 2 to 10. Adsorption decrease of MB under highly acidic conditions could be attributed to the presence of excess H^+ ions that competes with the cationic dye molecules for adsorption sites on the hydrogel nanocomposite. During adsorption, existence of anionic carboxylate and sulfate groups are necessary for interaction of the hydrogel nanocomposite with positively charged MB molecules. So, the increase in dye adsorption at basic solutions may be attributed to the strong electrostatic interactions between these negatively and positively charged groups that enhanced the adsorption capacity. With further increase in pH to a highly basic solution ($pH \geq 12$), however, adsorption capacity was decreased. The reason of the adsorption

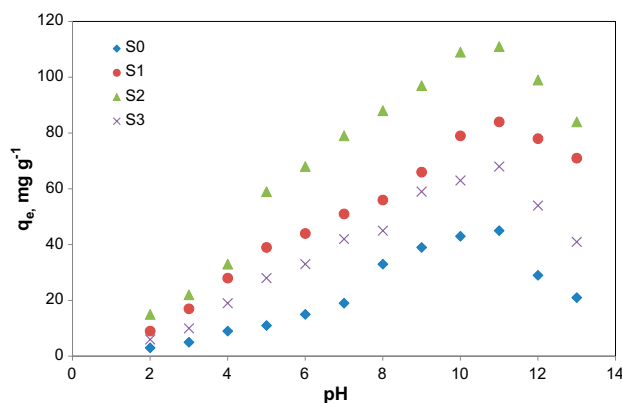


Fig. 5. Effect of pH of dye solution on MB adsorption.

loss for the highly basic solutions is “charge screening effect” of excess Na^+ in the adsorption media which shields the anionic functional groups and prevents effective negative–positive interactions of adsorbent and adsorbate.

It is necessary to mention that the pKa value of sulfate functional groups is -1.9 . So, these pendants functional groups in the hydrogel structure are completely dissociated in the overall pH range and therefore, show pH-independent swelling behavior [24]. In fact, in the overall pH range, these sulfate groups are in dissociated form. Therefore, the effects of pH on dye adsorption capacity were originated only by carboxylate functional groups of acrylic acid moieties. The pKa of the poly(acrylic acid) is 4.2. If the pH increases above 4.2, the carboxyl groups of the hydrogel nanocomposites become deprotonated, leading to strong charge repulsion between them. This leads to increase of the swelling capacity and therefore the dye adsorption ability of the nanocomposites.

3.4. Effect of adsorbent dose on dye adsorption capacity

In order to evaluate the effect of adsorbent dosage on MB removal, the amount of hydrogel nanocomposites (S1, S2, and S3) was varied from 20 up to 120 mg.

As shown in Fig. 6, the dye adsorption is increased when increasing the adsorbent dose until 80, 100, and 90 mg for S1, S2, and S3, respectively, and then begins to level off. Initial increment in dye adsorbent can be attributed to higher surface area and more availability of adsorption sites on the nanocomposites.

3.5. Effect of initial MB concentration on dye adsorption capacity

Various MB concentrations (10, 30, 60, 90, 120, and 150 mg L⁻¹) were used to depict the effect of initial dye concentration onto adsorption capability of the hydrogel nanocomposites. It is clear from Fig. 7 that the dye adsorption capacity increased initially with an increase in the MB concentration. This is attributed to the greater availability of dye molecules in the vicinity of the hydrogel nanocomposites. The increase in the dye concentration beyond 90 mg L⁻¹, however, did not affect significantly the adsorption capacity.

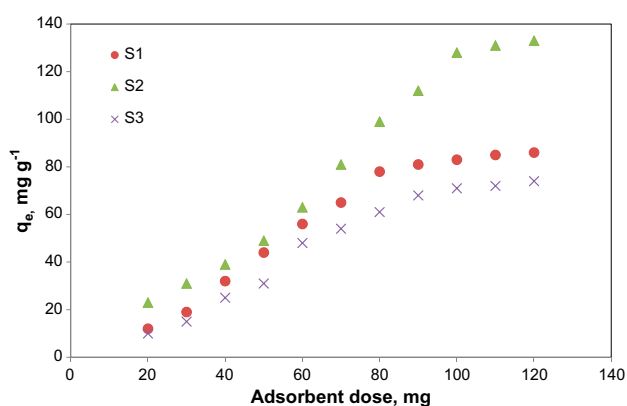


Fig. 6. Effect of adsorbent dosage on MB adsorption.

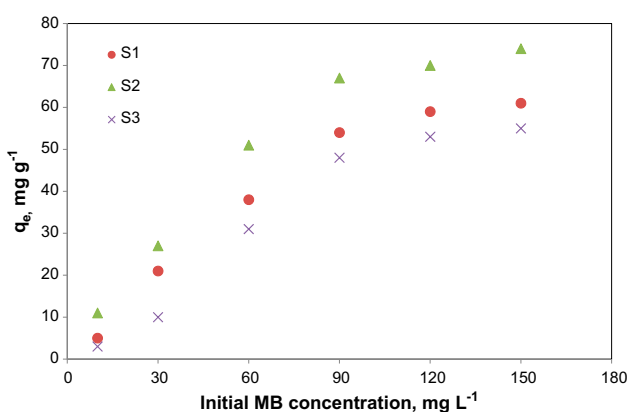


Fig. 7. Effect of initial dye concentration on MB adsorption.

3.6. Effect of temperature on dye adsorption capacity

The effect of temperature on removal of MB dye was carried out at four different temperatures (25, 35, 45, and 55°C). As shown in Fig. 8, the dye adsorption considerably increased with an increase in temperature for all samples. As temperature increases, the rate of MB diffusion within the hydrogel nanocomposite network increases, indicating that the adsorption process is endothermic.

In order to demonstrate this fact, the thermodynamic parameters including enthalpy (ΔH°), entropy (ΔS°), and change in free energy ΔG° have been calculated from the following equations [25]:

$$\ln K = \frac{\Delta S^\circ}{R} - \frac{\Delta H^\circ}{RT} \quad (2)$$

$$\Delta G^\circ = \Delta H^\circ - T\Delta S^\circ \quad (3)$$

where K equal to (q_e/C_e) is adsorption affinity, R is the gas constant ($8.314 \text{ J mol}^{-1} \text{ K}^{-1}$), and T is the temperature in Kelvin. The values of ΔH° and ΔS° are obtained from the slope and the intercept of the plot of $\ln K$ vs. $1/T$, respectively (Fig. 9 and Table 3). The ΔG° values are then calculated from Eq. (3). Results of the calculations are shown in Table 4. For all samples, the values of ΔG° at all temperatures are negative during the adsorption process. This confirms that the adsorption is thermodynamically favorable and spontaneous. The positive values of ΔH° and ΔS° also demonstrate that the adsorption is endothermic with probability of a favorable adsorption [26].

3.7. Adsorption isotherm modeling

Equilibrium relationships, generally known as bio-adsorption isotherms, are mathematical models which

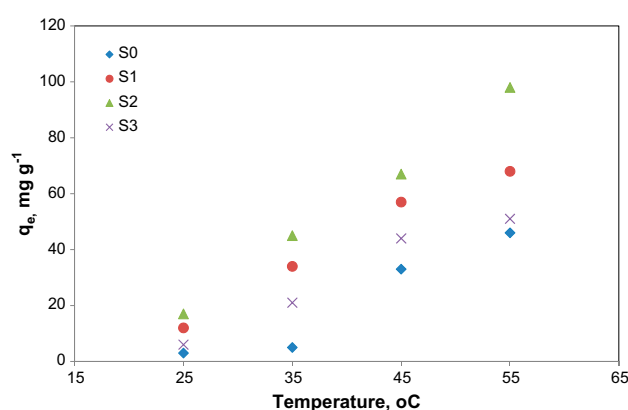


Fig. 8. Effect of temperature on MB adsorption.

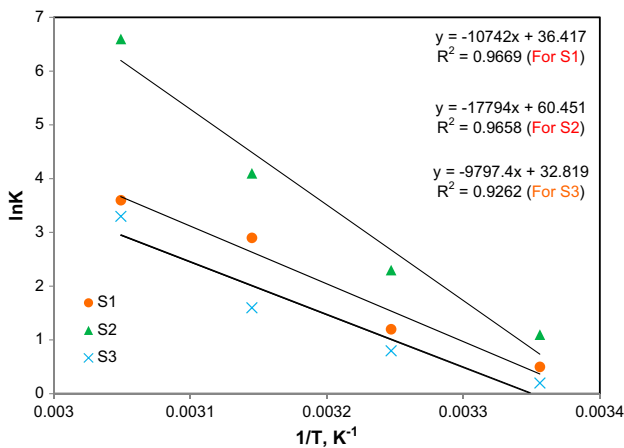


Fig. 9. Plot of $\ln K_L$ vs. $1/T$.

describe how adsorbates interact with adsorbents. Various adsorption isotherm models are available, and here we analyzed the experimental data according to the four nonlinear models: Langmuir, Freundlich, Temkin, and Redlich–Peterson. In this work, all the model parameters were calculated by nonlinear regression technique to avoid any linearization errors in the correlation coefficients (R^2).

The Langmuir model, the most widely used isotherm, assumes that adsorption occurs at specific homogenous sites of the adsorbent and all sites are equivalent. It is expressed as [27]:

$$\frac{C_e}{q_e} = \frac{1}{q_m K_L} + \frac{C_e}{q_m} \quad (4)$$

where C_e (mg L^{-1}) is the equilibrium concentration of MB solution and q_e is the amount of equilibrium adsorbed dye (mg g^{-1}). q_m (mg g^{-1}) is the theoretical maximum adsorption capacity and K_L (L mg^{-1}) are Langmuir isotherm constants. These constants could be determined from the slope and the intercept of the plot of C_e/q_e vs C_e (Fig. 10(A)). So, the maximum monolayer adsorption capacities were found to be 172.41, 192.31, and 153.85 mg g^{-1} for S1, S2, and S3, respectively. Results are tabulated in Table 5.

The Freundlich isotherm provides no information on the monolayer adsorption capacity. This model assumes neither homogenous sites nor limited levels of adsorption. The Freundlich isotherm equation has the following form [28]:

$$\ln q_e = \ln K_F + \left(\frac{1}{n}\right) \ln C_e \quad (5)$$

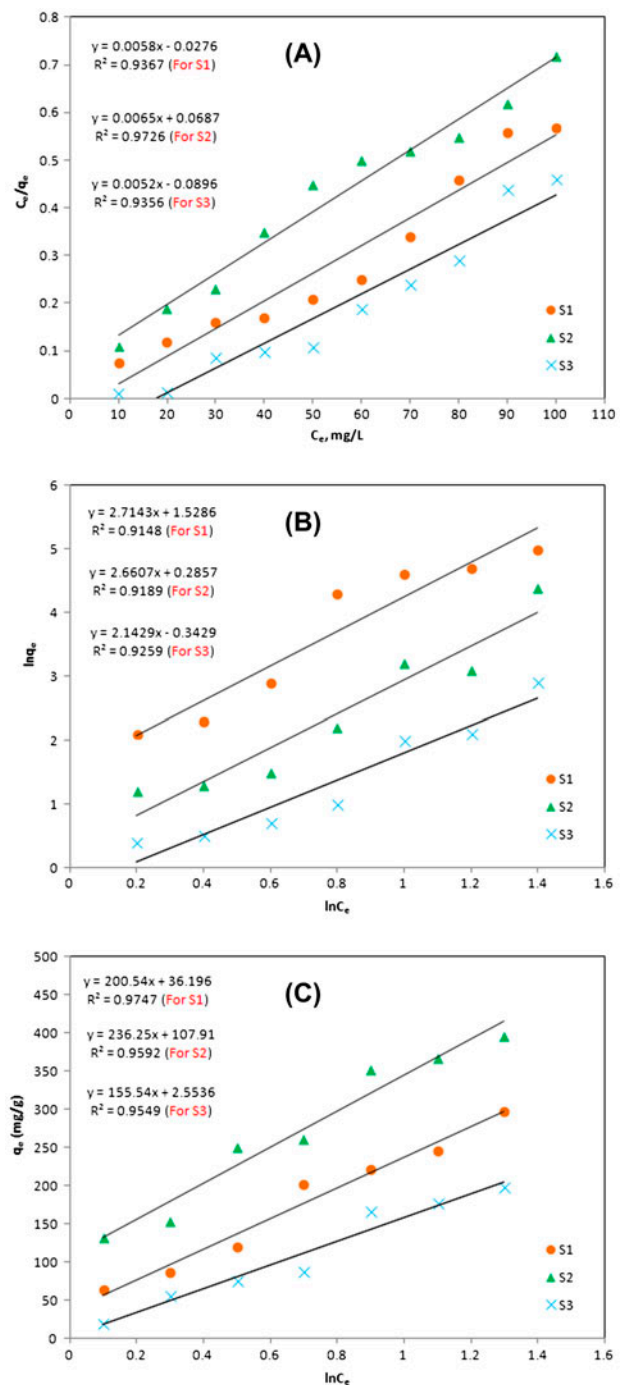


Fig. 10. The Langmuir (A), Freundlich (B), and Temkin (C) isotherm models for adsorption of MB onto the hydrogel nanocomposites.

where K_F and n are Freundlich constants which is related to the adsorption capacity and adsorption intensity, respectively. These constant values for nanocomposites can be achieved from the intercept

Table 3
 ΔH° and ΔS° for the adsorption of MB onto hydrogel nanocomposites

	S1	S2	S3
ΔH° (kJ mol ⁻¹)	44.2	55.8	63.1
ΔS° (J K ⁻¹ mol ⁻¹)	107.4	185.4	198.2

Table 4
 ΔG° values for the adsorption of MB onto hydrogel nanocomposites at various temperatures

T (K)	ΔG (kJ mol ⁻¹)		
	S1	S2	S3
298	-1.2	-2.5	-3.9
308	-1.9	-3.2	-4.5
318	-2.4	-4.3	-5.5
328	-3.4	-5.1	-7.4

Table 5
Parameters of the Langmuir, Freundlich, Temkin, and Redlich–Peterson isotherm models for adsorption of MB onto the hydrogel nanocomposites

Isotherms	Parameters	Hydrogel nanocomposite		
		S1	S2	S3
Langmuir	K_L	0.21	0.09	0.58
	q_m	172.41	192.31	153.85
	R^2	0.9367	0.9726	0.9356
Freundlich	K_F	36.24	54.91	44.52
	n	0.368	0.376	0.467
	R^2	0.9148	0.9189	0.9259
Temkin	K_T	1.632	2.465	0.894
	B	200.54	236.25	155.54
	R^2	0.9747	0.9592	0.9549
Redlich–Peterson	K_{RP}	0.936	2.451	1.344
	A	0.14	0.28	0.39
	R^2	0.997	0.999	0.995
$q_{e,exp}$ (mg g ⁻¹)		185	215	168

and the slope of $\ln q_e$ against $\ln C_e$ (Fig. 10(B) and Table 5).

The Temkin isotherm describes the indirect adsorbent/adsorbate interactions. This model expressed as follows [29]:

$$q_e = B \ln K_T + B \ln C_e \quad (6)$$

where B is the Temkin constant related to the heat of adsorption and K_T is the equation binding constant

related to the maximum binding energy. From the slope and the intercept of the plot q_e vs. $\ln C_e$ (Fig. 10(C)), we could be obtained the Temkin constants as shown in Table 5.

Finally, the Redlich–Peterson isotherm uses three parameters by combining elements from both the Langmuir and Freundlich isotherms. In this model, the adsorption mechanism does not follow ideal monolayer adsorption and can describe the adsorption process over a wide range of concentrations [30]. It can be represented by the following formula [31]:

$$q_e = \frac{K_{RP} C_e}{1 + A C_e^b} \quad (7)$$

where K_{RP} (L g⁻¹) and A ((L mg⁻¹)^b) are Redlich–Peterson constants, and b is the isotherm exponent indicating the heterogeneity of the adsorbent ranging between 0 and 1. The adsorbent parameters of this model are also listed in Table 5.

The fits of experimental data to the above mentioned isotherm models were finally evaluated by the nonlinear coefficients of determination (R^2). The values of R^2 for all isotherm models are also presented in Table 5. The R^2 values depict that Redlich–Peterson isotherm (from 0.997 to 0.999) has the best correlation to the experimental data than the other models (from 0.9148 to 0.9747). The R^2 values of both the Langmuir and Redlich–Peterson models, however are greater than the Freundlich model, which implies that the adsorption isotherm follows monolayer adsorption (for $b=1$, the Redlich–Peterson equation reduces to Langmuir form). Moreover, the results in Fig. 11 indicate that the Redlich–Peterson isotherm best fits the experimental data (difference of $q_{measured} - q_{model}$) for MB adsorption on S2 sample. In this figure, the theoretical plots for all isotherms have been compared with the experimental data.

3.8. Adsorption kinetics

One of the most important parameters to evaluate the adsorption efficiency of adsorbent materials is kinetic of dye removal. In fact, it is very important to understand kinetics of adsorption process for practical applications including process design and scale-up procedures. In order to investigate the adsorption kinetics and to study the time dependence of adsorption process and further investigate the adsorption mechanisms, various models have been used. In this study, we used three well-known kinetic models, i.e. pseudo-first-order, pseudo-second-order, and intra-particle to fit the adsorption date.

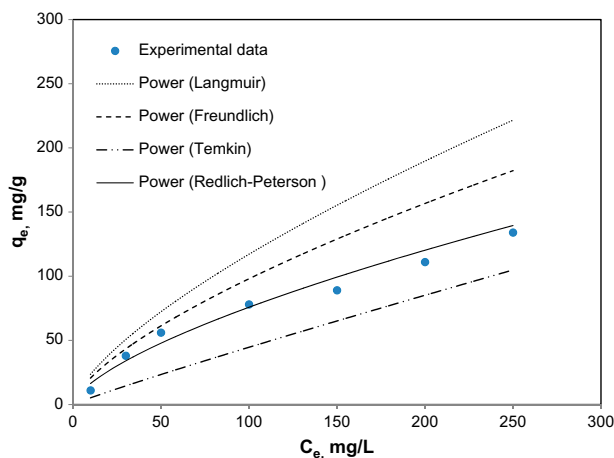


Fig. 11. Comparison of the adsorption equilibrium isotherms of MB onto the hydrogel nanocomposite (S2 sample) with the experimental points.

The pseudo-first-order rate equation is given by the following equation [32]:

$$\ln(q_e - q_t) = \ln q_{e1} - k_1 t \quad (8)$$

where q_e and q_t are the amounts of dye adsorbed at equilibrium (mg g^{-1}) and at contact time t (min), respectively. q_{e1} and k_1 show the theoretical equilibrium adsorption and rate constant of pseudo-first-order kinetic model, respectively. The values k_1 and q_{e1} can be determined from the slope and the intercept of the plot of $\ln(q_e - q_t)$ against t (Fig. 12(A)) and presented in Table 6.

The rate of the pseudo-second-order model depends on the amount and the quantity of dye adsorbed on the surface of adsorbent [33]. The pseudo-second-order rate can be expressed as follows [34]:

$$\frac{t}{q_t} = \frac{1}{k_2(q_{e2})^2} + \frac{t}{q_{e2}} \quad (9)$$

where k_2 ($\text{g mg}^{-1} \text{min}^{-1}$) is the pseudo-second-order rate constant and q_{e2} is the theoretical adsorbed dye (mg g^{-1}). In this case, the slope and the intercept of the plot t/q_e vs. t (Fig. 12(B)) gives k_2 and q_{e2} values as presented in Table 6.

Else, the initial biosorption rate, h ($\text{mg g}^{-1} \text{min}^{-1}$), is assessed by Eq. (10):

$$h = k_2 (q_{e2})^2 \quad (10)$$

The aforementioned kinetic models could not describe the biosorption diffusion mechanism. So, the intra-particle diffusion was also used as expressed by Eq. (11) [35]:

$$q_t = k_{id} t^{1/2} + c \quad (11)$$

where c is the intercept (mg g^{-1}) and k_{id} ($\text{mg g}^{-1} \text{min}^{-1/2}$) is the intra-particle diffusion rate constant, which can be obtained from the slope of the plot of q_t vs. $t^{1/2}$ (Fig. 12(C)). The obtained k_p and c values are also shown in Table 6. In Eq. (11), c is the intra-particle diffusion constant, which is directly proportional to the boundary layer thickness.

According to Fig. 12 and Table 6, it is revealed that for all samples a good agreement of the theoretical adsorption capacity with the experimental data are obtained by using the pseudo-second-order kinetic model as the correlation coefficients (R^2) are closer to 1 than those of kinetic models. For the pseudo-second-order model, this coefficient varies from 0.9966 to 0.9997. Moreover, the q_{e2} values for the second-order kinetic is closer to the experiments ($q_{e,exp}$). So, this set shows that the rate-limiting step is likely the surface adsorption for the dye removal process by a chemical sorption involving valence forces between adsorbent and adsorbate [36].

For the pseudo-first-order model, however, the low correlation coefficients (from 0.9377 to 0.9564) suggested the poor agreement of pseudo-first-order kinetics with the experimental data. Moreover, the plot for

Table 6

Kinetic parameters of the pseudo-first-order, pseudo-second-order, and intra-particle models for MB adsorption by the hydrogel nanocomposites

	Pseudo-first-order			Pseudo-second-order			Intra-particle			$q_{e,exp}$
	k_1	q_{e1}	R^2	k_2	q_{e2}	R^2	k_{id}	R^2	c	
S1	0.011	122	0.9377	0.003	182	0.9997	2.57	0.9489	-7.4	185
S2	0.015	155	0.9564	0.007	209	0.9971	3.01	0.9613	+9.1	215
S3	0.013	105	0.9518	0.009	161	0.9966	2.21	0.9571	-16.1	168

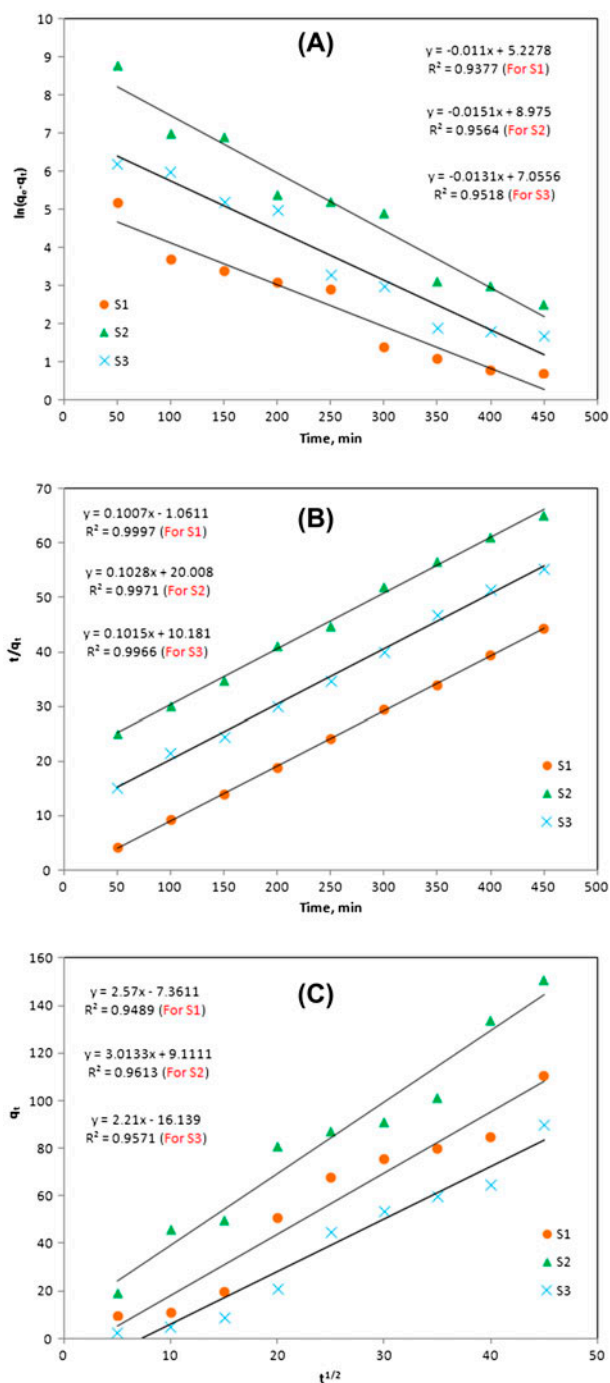


Fig. 12. Adsorption kinetics of MB adsorption by the hydrogel nanocomposites according to the pseudo-first-order (A), pseudo-second-order (B), and intra-particle (C) models.

the intra-particle diffusion model (Fig. 12(C)) did not pass through the origin implying that the intra-particle diffusion was not the rate-limiting step.

4. Conclusions

In this work, the efficient adsorption of MB dye from aqueous solutions using a novel anionic hydrogel nanocomposite was studied and the following main results were obtained:

- (1) It was observed that the specific interactions between cationic dye and anionic monomers in the hydrogel network affected the dye binding capability of the hydrogel nanocomposite.
- (2) The maximum dye adsorption capacity (215 mg g^{-1}) was achieved under the optimum conditions that found to be: Agitation time 120 min, MMT content 0.5 g, pH 10, initial dye concentration 90 mg L^{-1} , adsorbent dose 100 mg, and temperature 55°C .
- (3) Thermodynamic parameters indicate that the dye adsorption is spontaneous and endothermic in nature.
- (4) The adsorption of MB onto the hydrogel nanocomposites fitted well with the Redlich–Peterson isotherm model.
- (5) The sorption data were also demonstrated that the adsorption of MB follows pseudo-second-order kinetics.

Overall, this novel hydrogel nanocomposite adsorbent with a satisfying adsorption capacity, high adsorption rate, simple preparation method, and finally low production cost can be used for removal of various cationic dyes from aqueous solutions.

References

- [1] G. Crini, Recent developments in polysaccharide-based materials used as adsorbents in wastewater treatment, *Prog. Polym. Sci.* 30 (2005) 38–70.
- [2] R. Sanghi, B. Bhattacharya, Review on decolorization of aqueous dye solutions by low cost adsorbents, *Color. Technol.* 118 (2002) 256–269.
- [3] G.L. Dotto, L.A.A. Pinto, Adsorption of food dyes onto chitosan: Optimization process and kinetic, *Carbohydr. Polym.* 84 (2011) 231–238.
- [4] G.R. Mahdavinia, S. Irvani, S. Zoroufi, H. Hosseinzadeh, Magnetic and K^+ -cross-linked kappa-carrageenan nanocomposite beads and adsorption of crystal violet, *Iran. Polym. J.* 23 (2014) 335–344.
- [5] A. Pourjavadi, S.H. Hosseini, F. Seidi, R. Soleyman, Magnetic removal of crystal violet from aqueous solutions using polysaccharide-based magnetic nanocomposite hydrogels, *Polym. Int.* 62 (2012) 1038–1044.
- [6] K.P. Singh, S. Gupta, A.K. Singh, S. Sinha, Optimizing adsorption of crystal violet dye from water by magnetic nanocomposite using response surface modeling approach, *J. Hazard. Mater.* 186 (2011) 1462–1473.

- [7] K. Mohanty, J.T. Naidu, B.C. Meikap, M.N. Biswas, Removal of crystal violet from wastewater by activated carbons prepared from rice husk, *Ind. Eng. Chem. Res.* 45 (2006) 5165–5171.
- [8] K. Sui, Y. Li, R. Liu, Y. Zhang, X. Zhao, H. Liang, Y. Xia, Biocomposite fiber of calcium alginate/multi-walled carbon nanotubes with enhanced adsorption properties for ionic dyes, *Carbohydr. Polym.* 90 (2012) 399–406.
- [9] P. Sharma, H. Kaur, M. Sharma, V. Sahore, A review on applicability of naturally available adsorbents for the removal of hazardous dyes from aqueous waste, *Environ. Monit. Assess.* 183 (2011) 151–195.
- [10] F.L. Buchholz, A.T. Graham, *Modern Superabsorbent Polymer Technology*, Wiley, New York, NY, 1997.
- [11] L. Sorbara, L. Jones, L.D. Williams, Contact lens induced papillary conjunctivitis with silicone hydrogel lenses, *Contact. Len. Anter. Eye* 32 (2009) 93–96.
- [12] C.T. Lee, P.H. Kung, Y.D. Lee, Preparation of poly (vinyl alcohol)chondroitin sulfate hydrogel as matrices in tissue engineering, *Carbohydr. Polym.* 61 (2005) 348–354.
- [13] J. Wu, W. Wei, Y.W. Lian, Z.G. Su, G.H. Ma, A thermosensitive hydrogel based on quaternized chitosan and poly(ethylene glycol) for nasal drug delivery system, *Biomaterials* 28 (2007) 2220–2232.
- [14] K. Haraguchi, T. Takehisa, Nanocomposite hydrogels: A unique organic–inorganic network structure with extraordinary mechanical, optical, and swelling/deswelling properties, *Adv. Mater.* 14 (2002) 1120–1124.
- [15] K. Haraguchi, T. Takehisa, S. Fan, Effects of clay content on the properties of nanocomposite hydrogels composed of poly(N-isopropylacrylamide) and clay, *Macromolecules* 35 (2002) 10162–10171.
- [16] W.A. Zhang, W. Luo, Y.E. Fang, Synthesis and properties of a novel hydrogel nanocomposite, *Mater. Lett.* 59 (2005) 2876–2880.
- [17] X. Yuanqing, P. Zhiqin, A new polymer/clay nanocomposite hydrogel with improved response rate and tensile mechanical properties, *Eur. Polym. J.* 42 (2006) 2125–2132.
- [18] Q. Zhang, X. Li, Y. Zhao, L. Chen, Preparation and performance of nanocomposite hydrogels based on different clay, *Appl. Clay Sci.* 46 (2009) 346–350.
- [19] G. Bagheri Marandi, G.R. Mahdavinia and S. Ghafary, Collagen-g-poly (sodium acrylate-co-acrylamide)/sodium montmorillonite superabsorbent nanocomposites: Synthesis and swelling behavior, *J. Polym. Res.* 18 (2011) 1487–1499.
- [20] M. Sirousazar, M. Kokabi, Z.M. Hassan, Swelling behavior and structural characteristics of polyvinyl alcohol/montmorillonite nanocomposite hydrogels, *J. Appl. Polym. Sci.* 123 (2012) 50–58.
- [21] G. Crini, P.M. Badot, Application of chitosan, a natural aminopolysaccharide, for dye removal from aqueous solutions by adsorption processes using batch studies: A review of recent literature, *Prog. Polym. Sci.* 33 (2008) 399–447.
- [22] F. Santiago, A.E. Mucientes, M. Osorio, C. Rivera, Preparation of composites and nanocomposites based on bentonite and poly(sodium acrylate). Effect of amount of bentonite on the swelling behavior, *Eur. Polym. J.* 43 (2007) 1–9.
- [23] A. Li, A. Wang, Synthesis and properties of clay-based superabsorbent composite, *Eur. Polym. J.* 41 (2005) 1630–1637.
- [24] S. Durmaz, O. Okay, Acrylamide/2-acrylamido-2-methylpropane sulfonic acid sodium salt-based hydrogels: Synthesis and characterization, *Polymer* 41 (2000) 3693–3704.
- [25] E. Daneshvara, M. Koushaa, M. Jokarb, N. Koutahzadehb, E. Guibal, Acidic dye biosorption onto marine brown macroalgae: Isotherms, kinetic and thermodynamic studies, *Chem. Eng. J.* 204–206 (2012) 225–234.
- [26] K.P. Singh, D. Mohan, S. Sinha, G.S. Tondon, D. Gosh, Color removal from wastewater using low-cost activated carbon derived from agricultural waste material, *Ind. Eng. Chem. Res.* 42 (2003) 1965–1976.
- [27] A.E. Ofomaja, E.I. Unuabonah, Kinetics and time-dependent Langmuir modeling of 4-nitrophenol adsorption onto *Mansonia* sawdust, *J. Taiwan Inst. Chem. Eng.* 44 (2013) 566–576.
- [28] B.K. Nandi, A. Goswami, A.K. Das, B. Mondal, M.K. Purkait, Kinetic and equilibrium studies on the adsorption of crystal violet dye using kaolin as an adsorbent, *Sep. Sci. Technol.* 43 (2008) 1382–1403.
- [29] M.I. Temkin, V. Pyzhev, Kinetics of ammonia synthesis on promoted iron catalysts, *Acta Physicochim.* 12 (1940) 327–356.
- [30] A.A. Oladipo, M. Gazi, S. Saber-Samandari, Adsorption of anthraquinone dye onto eco-friendly semi-IPN biocomposite hydrogel: Equilibrium isotherms, kinetic studies and optimization, *J. Taiwan Inst. Chem. Eng.* 45 (2014) 653–664.
- [31] K.Y. Foo, B.H. Hameed, Insights into the modeling of adsorption isotherm systems, *Chem. Eng. J.* 156 (2010) 2–10.
- [32] A. Mittal, J. Mittal, A. Malviya, V.K. Gupta, Adsorptive removal of hazardous anionic dye “Congo red” from wastewater using waste materials and recovery by desorption, *J. Colloid Interface Sci.* 340 (2009) 16–26.
- [33] A. Gucek, S. Sener, S. Bilgen, M.L. Mazmanci, Adsorption and kinetic studies of cationic and anionic dyes on pyrophyllite from aqueous solutions, *J. Colloid Interfaces Sci.* 286 (2005) 53–60.
- [34] V.K. Gupta, A. Rastogi, A. Nayak, Biosorption of nickel onto treated alga (*Oedogonium hatei*): Application of isotherm and kinetic models, *J. Colloid Interface Sci.* 342 (2010) 533–539.
- [35] K. Kannan, M.M. Sundaram, Kinetics and mechanism of removal of methylene blue by adsorption on various carbons—A comparative study, *Dyes Pigm.* 51 (2001) 25–40.
- [36] P.D. Saha, S. Chakraborty, S. Chowdhury, Batch and continuous (fixed-bed column) biosorption of crystal violet by *Artocarpus heterophyllus* (jackfruit) leaf powder, *Colloids Surf. B* 92 (2012) 262–270.
- [37] M. Belhachemi, F. Addoun, Adsorption of congo red onto activated carbons having different surface properties: Studies of kinetics and adsorption equilibrium, *Desalin. Water Treat.* 37 (2012) 122–129.
- [38] M.C. Shih, Kinetics of the batch adsorption of methylene blue from aqueous solutions onto rice husk: Effect of acid-modified process and dye concentration, *Desalin. Water Treat.* 37 (2012) 200–214.
- [39] M. Topcu Sulaka, H. Cengiz Yatmazb, Removal of textile dyes from aqueous solutions with eco-friendly biosorbent, *Desalin. Water Treat.* 37 (2012) 169–177.

- [40] C. Weng, Y. Pan, Adsorption characteristics of methylene blue from aqueous solution by sludge ash, *Colloids Surf., A* 274 (2006) 154–162.
- [41] M. Arami, N.Y. Limaee, N.M. Mahmoodi, N.S. Tabrizi, Removal of dyes from colored textile wastewater by orange peel adsorbent: Equilibrium and kinetic studies, *J. Colloid Interface Sci.* 288 (2005) 371–376.
- [42] G. Annadurai, R. Juang, D. Lee, Use of cellulose based wastes for adsorption of dyes from aqueous solutions, *J. Hazard. Mater.* B92 (2002) 263–274.
- [43] T. Akar, I. Tosun, Z. Kaynak, E. Ozkara, O. Yeni, E.N. Sahin, S.T. Akar, An attractive agro-industrial by-product in environmental cleanup: Dye biosorption potential of untreated olive pomace, *J. Hazard. Mater.* 166 (2009) 1217–1225.
- [44] B.H. Hameed, Removal of cationic dye from aqueous solution using jackfruit peel as a non-conventional and low-cost adsorbent, *J. Hazard. Mater.* 162 (2009) 344–350.
- [45] B. Bestani, N. Benderdouche, B. Benstaali, M. Belhakem, A. Addou, Methylene blue and iodine adsorption onto an activated desert plant, *Bioresour. Technol.* 99 (2008) 8441–8444.
- [46] A.E. Ofomaja, Kinetic study and sorption mechanism of methylene blue and methyl violet onto mansonia (*Mansonia altissima*) wood sawdust, *Chem. Eng. J.* 143 (2008) 85–95.
- [47] G.C. Panda, S.K. Das, A.K. Guha, Jute stick powder as a potential biomass for the removal of Congo red and rhodamine B from their aqueous solution, *J. Hazard. Mater.* 164 (2008) 374–379.
- [48] F. Ferrero, Dye removal by low cost adsorbent: Hazelnut shells in comparison with wood sawdust, *J. Hazard. Mater.* 142 (2007) 144–152.
- [49] M. Alkan, S. Celikcapa, O. Demirbas, M. Dogan, Removal of reactive blue 221 and acid blue 62 anionic dyes from aqueous solutions by sepiolite, *Dyes Pigm.* 65 (2005) 251–259.
- [50] O. Ozdemir, B. Armagan, M. Turan, M.S. Celik, Comparison of the adsorption characteristics of azo-reactive dyes on mesoporous minerals, *Dyes Pigm.* 62 (2004) 49–60.
- [51] M. Dogan, M. Alkan, Removal of methyl violet from aqueous solution by perlite, *J. Colloid Interface Sci.* 267 (2003) 32–41.
- [52] E. Eren, Removal of basic dye by modified Unye bentonite, Turkey, *J. Hazard. Mater.* 162 (2009) 1335–1363.
- [53] A.A. Oladipo, M. Gazi, Enhanced removal of crystal violet by low cost alginate/acid activated bentonite composite beads: Optimization and modeling using non-linear regression technique, *J. Water Process Eng.* 2 (2014) 43–52.
- [54] S. Zhao, F. Zhou, L. Li, M. Cao, D. Zuo, H. Liu, Removal of anionic dyes from aqueous solutions by adsorption of chitosan-based semi-IPN hydrogel composites, *Composites: Part B* 43 (2012) 1570–1578.
- [55] G. Akkaya, I. Uzun, F. Guzel, Kinetics of the adsorption of reactive dye by chitin, *Dyes Pigm.* 73 (2007) 168–177.